

INVESTIGATION OF DOUBLE GAUSSIAN DISTRIBUTION MODEL OF Au/FREE STANDING GaN SCHOTTKY CONTACT GROWN BY HVPE

M. I.ARSHAD^a, A.ALI^a, M. ASGHAR^b, M. AJAZ-UN -NABI^a,N. AMIN^a,
K.MAHMOOD^{a*}

^aDepartment of Physics, GC University Faisalabad, 38000, Pakistan

^bDepartment of Physics, The Islamia University of Bahawalpur, 63100, Pakistan

In this paper, we have investigated the current-voltage (I-V) characteristics of Au Schottky diode fabricated on free standing GaN (FS GaN) grown by HVPE in the temperature of 160-450K. The temperature dependent ideality factor and barrier height were calculated from the semi-logarithmic current-voltage (I-V) characteristics with room temperature values 2.60 ± 0.01 and 0.55 ± 0.01 eV respectively. The strong temperature dependence of experimental barrier height and ideality factor demonstrated the inhomogeneity at Au/FS GaN interface. This inhomogeneous behavior was modeled by assuming the existence of a two sets of Gaussian distribution (Region I and II) of barrier heights in temperature range of 160-240 K and 240-450 K respectively. The weighting coefficients for each Gaussian distribution and their standard deviations were found to be 1.41 ± 0.01 eV- 0.048 ± 0.001 eV and 0.741 ± 0.01 eV- 0.013 ± 0.001 eV for distribution region I and II respectively. The values for barrier height and Richardson constant also have been calculated as 1.2 eV, 21.4 $\text{AK}^{-2}\text{cm}^{-2}$ and 0.7 eV, 25.4 $\text{AK}^{-2}\text{cm}^{-2}$ from the modified Richardson plot for the respective temperature region. The calculated A^* value is close agreement with the standard value ($26 \text{AK}^{-2}\text{cm}^{-2}$) for n-GaN. It has been shown that these results supported the presence of double Gaussian distribution model of barrier height inhomogeneities in the temperature range of 160 to 450 K.

(Received March 7, 2015; Accepted June 22, 2015)

Keywords: Free standing GaN: I-V Characteristics: Barrier height:

Double Gaussian distribution

1. Introduction

GaN is very promising material for electronic, high power and high frequency device applications [1-3] due to its amazing properties like wide band gap, high break down field and high electron saturation velocity [4, 5]. Due to these remarkable properties, GaN emerges as potential candidate for light emitting diodes, laser diodes, high electron mobility transistors and field effect transistors [6-8]. In order to use these devices for commercial applications, the investigation of transport mechanism and contact behavior has fundamental importance. It is reported that room temperature current-voltage characteristics of Schottky barrier diodes usually deviate from the ideal thermionic model due to the strong dependence of both barrier height and ideality factor on temperature and nonlinearity of the Richardson plots [9-11]. This observed non-ideal behavior of Schottky barriers has been attributed to the inhomogeneity at the interface of metal and GaN. Many authors have reported this inhomogeneous behavior of Schottky diode [12-16]; For example; Reddy et al [12] investigated the temperature dependent electrical characteristics of Se/n-GaN Schottky barrier diodes in the temperature range of 130-400K. They observed the double Gaussian distribution of inhomogeneous barrier heights in Se/n-GaN Schottky diodes. M. Siva et al [13] suggested that Ni/Pd/n-GaN Schottky diode can be explained by assuming the existence of double

* Corresponding author: khalid_mahmood856@yahoo.com

Gaussian distribution of the Schottky barrier heights in the wide temperature range. Huang et al [14] demonstrated the current transport mechanism in Au/Ni/n-GaN Schottky diodes using I-V in the temperature range 27-350 °C. They reported that thermionic emission model with a Gaussian distribution of Schottky barrier diode (SBD) is thought to be responsible for the electrical behavior at lower temperature, while the generation recombination process takes place at temperature above 230 °C. But no report has been found on the double Gaussian distribution inhomogeneity of Au Schottky contact on free standing n-GaN grown by HVPE in the literature, according to best of our knowledge. Therefore a detailed study to investigate the contact properties of Au Schottky diodes on free standing GaN is still open and additional works are required to understand the electrical transport mechanism in Au/FS GaN Schottky diodes.

In this paper, we have investigated the I-V characteristics of Au Schottky contact on free standing GaN in the temperature range of 150-450K. The measured values of temperature dependent ideality factor and barrier height suggested that ideality factor decreases and barrier height increases as temperature increases. Furthermore, we observed a linear relationship between ideality factor and barrier height. These anomalies have been explained by thermionic emission mechanism by assuming the coexistence of double Gaussian distributions of barrier heights of Au metal contact on free standing n-GaN.

2. Experimental

Free-standing GaN samples were grown in a hydride vapor phase reactor of horizontal configuration. The precursors employed for the growth process were gallium (Ga) melt, which was flushed with HCl flow at 1000 °C to form gallium chloride (GaCl) species. These GaCl species reacted with gaseous ammonia (NH₃) over the sapphire substrate to form GaN. To grow directly on the sapphire substrate, it is necessary to first deposit a GaN nucleation layer at a pressure of 200 mbar and at a temperature of 600 °C with a V/III ratio of 100, preceding the epitaxial growth step, performed at an elevated temperature of 1070 °C and pressure of 970 mbar with an average growth rate of 250 μm⁻¹. Thick GaN layers of 500 μm were grown in successive series of two runs. During the cooling down of the samples after the second growth run, the GaN layers were spontaneously separated into pieces from the sapphire substrate due to built-in high thermal strain. Often as-grown, free-standing HVPE GaN layers exhibit background doping of n-type. This is because the growth under extreme conditions results in an incorporation of impurities such as Si and O from the corroding quartz reactor tube. The detail growth and metalization process is described in reference [17]. As-grown layers were characterized for crystalline quality and structural defects by characterization techniques such as x-ray diffraction and photoluminescence, which confirmed the hexagonal structure of grown layers. The Schottky contacts of 1 mm diameter were deposited by evaporating Au metal using electron beam evaporation system. The temperature dependent I-V measurements of the Au/n-FS GaN Schottky diodes were performed by automated deep level transient spectrometer (SEMILAB DLS-83). The device temperature was controlled with accuracy of ±1 K by temperature controller DLS-83D cryostat

3. Results and discussion

The current flow through the Schottky barrier diode can be explained by the thermionic emission theory. The I-V relationship of diode, neglecting series resistance is given as [18],

$$I = I_s \left[\exp\left(\frac{qV}{nkT}\right) - 1 \right] \quad (1)$$

Where n is the ideality factor and I_s is the reverse saturation current given by the relation,

$$I_s = AA^*T^2 \exp\left[\frac{-q\phi_B}{kT}\right] \quad (2)$$

Where A is the contact area, A^* is the Richardson constant and its value is $26 \text{ AK}^{-2} \text{ cm}^{-2}$ for n-GaN [19]. T is temperature in Kelvin, k is the Boltzmanns constant ($k= 8.617 \times 10^{-5} \text{ eV/K}$), q is the electric charge and ϕ_B is the barrier height.

The ideality factor n at different temperatures was calculated by the slope $\frac{q}{nkT}$ of semi-log plot of the forward bias I–V curve (fig. 1) by using the relation,

$$n = \frac{q}{kT \times \text{slope}} \quad (3)$$

The semi-log plot of the (I–V) curve (fig.1) was used to calculate the barrier height $\phi_B(I-V)$ by using the following relation [20],

$$\phi_{B(I-V)} = \frac{kT}{q} \ln\left(\frac{AA^*T^2}{I_s}\right) \quad (4)$$

Where $k=8.617 \times 10^{-5} \text{ eV/K}$, T is the temperature in Kelvin, A is the contact area $=0.78 \text{ mm}^2$ and A^* is the Richardson constant having value $26 \text{ AK}^{-2} \text{ cm}^{-2}$ for n-GaN [21].

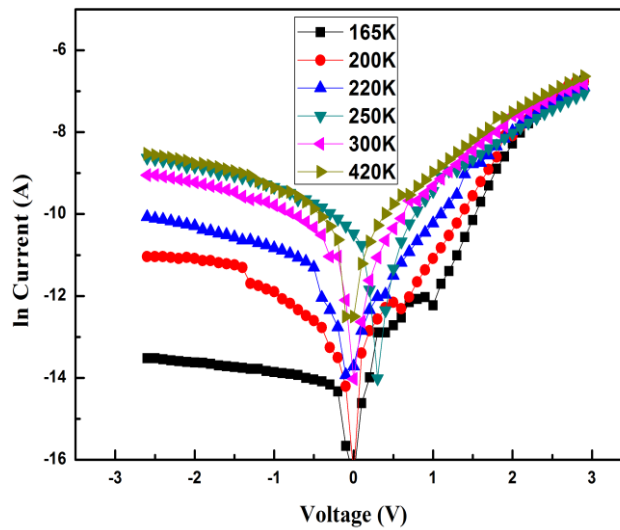


Fig. 1 Semi log forward biased I–V characteristics of Au/n-FS GaNSchottky barrier diode in the temperature range of 160 -450 K.

The high values of ideality factor at low temperatures may be due to the presence of excess current, potential drop in the interfacial layer and the recombination current through the interfacial states of the junction. The calculated room temperature values of n and BH for Au/FS GaNSchottky diode are 2.60 ± 0.01 and $0.55 \pm 0.01 \text{ eV}$ respectively. The detail of estimated values at different temperatures can be seen in table 1. The variation of ideality factor and barrier heights with temperature are demonstrated in fig.2. It is observed that ideality factor decreases and barrier height increases with increasing temperature. The temperature dependence behavior of ideality factor and barrier height indicates the inhomogenous nature of Schottky barrier height [22, 23].

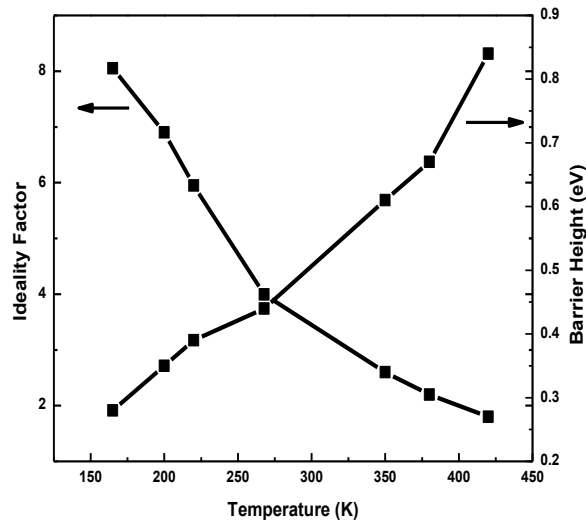


Fig. 2 Plot of ideality factor and barrier height versus temperature for Au/n-FS GaNSchottky diode.

Table 1. Effect of temperature on ideality factor, barrier height and saturation current

| Temperature (K) | Barrier Height (eV) | Ideality Factor (n) | Saturation Current (A) |
|-----------------|---------------------|---------------------|------------------------|
| 165 | 0.28939 | 8.05394 | 1.1E-6 |
| 200 | 0.3549 | 6.90376 | 1.2E-6 |
| 220 | 0.39251 | 5.95486 | 1.35E-6 |
| 250 | 0.44779 | 3.91008 | 1.35E-6 |
| 350 | 0.61624 | 2.40827 | 1.8E-6 |
| 380 | 0.67302 | 2.07288 | 2.0E-6 |
| 420 | 0.84425 | 1.76425 | 2.2E-6 |

Fig. 3 shows a plot of ideality factor and barrier height for Au/FS GaNSchottky diode. This straight line plot indicates a linear relationship between experimental effective barrier height and ideality factor of Schottky diodes. Again, the decrease of ideality factor and increase of barrier height with increasing temperature shows a discontinuity at the Au/FS GaN interface. Similar results have been reported in the literature [24, 25]. The graph in figure 3 demonstrated that there are two linear regions between experimental zero-biased BH and ideality factor, which can be explained by lateral inhomogeneities of BH. The extrapolation of experimental barrier height and ideality factor plot for $n=1$ gives mean values of barrier heights 0.99 and 0.87 eV for region I and II respectively.

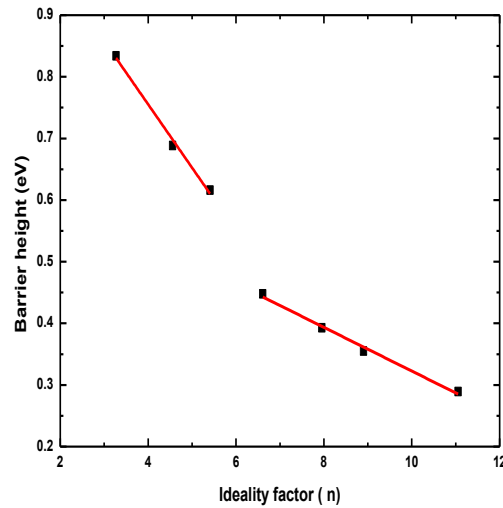


Fig. 3 Schottky barrier heights versus ideality factor of the Au/n-FS GaNSchottky barrier diode in the temperature range of 160–450 K

This barrier height inhomogeneity can be explained by using Gaussian distribution model of barrier height. According to this model, the barrier height can be written as [26]

$$\varphi_{ap} = \varphi_{bo} - \frac{q\sigma_s^2}{2kT} \quad (5)$$

where φ_{ap} is the apparent BH which can be measured experimentally, φ_{bo} is the mean BH and φ_s is the standard deviation of the BH distribution. The standard deviation is the measure of barrier homogeneity. The temperature dependence of φ_s is usually small and can be neglected.

In this model the observed variation of ideality factor with temperature is given by [27]

$$\frac{1}{n_{ap}} = -\rho_2 + \frac{q\rho_3}{2kT} \quad (6)$$

where n_{ap} is the apparent ideality factor and ρ_2 and ρ_3 are voltage coefficients which may depend on temperature and they quantify the voltage deformation of the BH distribution.

Fig. 4 shows a plot between φ_{ap} and $1/2kT$ for Au/FS GaNSchottky diode. The figure 4 demonstrated that there are two straight lines instead of single line which indicates the presence of double Gaussian distribution at the interface [28]. Furthermore, the linear relationship between barrier height and $1/2kT$ shows that temperature dependent Au/FS GaN I-V data is in agreement with Gaussian distribution model [29, 30]. The intercept and slope of this plot gives the mean barrier height and the zero-bias standard deviation with values 1.31 ± 0.01 , 0.741 ± 0.01 eV and 0.048 ± 0.001 , 0.013 ± 0.001 eV for distribution I and II respectively. The inhomogeneity of the interface depends upon the value of standard deviation i.e lower value of standard deviation corresponds to more homogeneous barrier heights.

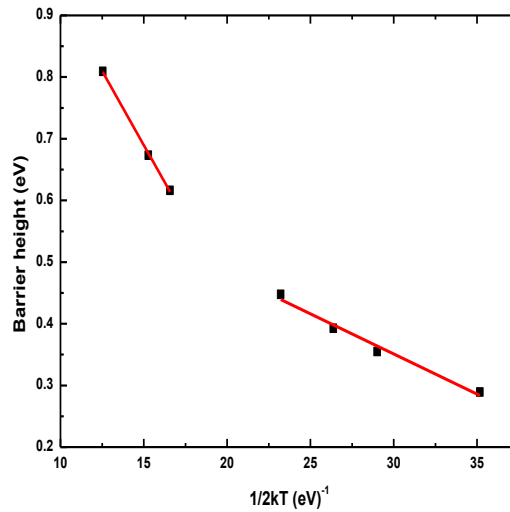


Fig. 4 Zero-bias apparent barrier height versus $1/(2kT)$ curves of the Au/n-FS GaNSchottky diode according to two Gaussian distributions of BHs. The data show linear variation in the two temperatureranges with a transition around 240 K.

The plot of $(1/n_{ap}-1)$ versus $1/2kT$ is again has linear relationship with two distributions shown in fig. 5. The values of voltage coefficients ρ_2 and ρ_3 can be calculated from the intercept and slope of this graph. The values of ρ_2 obtained from the intercept of experimental n_{ap} versus $1/2kT$ curve are 1.06 ± 0.01 eV for region I and -0.11 ± 0.01 eV for region II while the values of ρ_3 obtained from the slope are -0.74 ± 0.01 eV and 0.0049 eV for region I and II respectively.

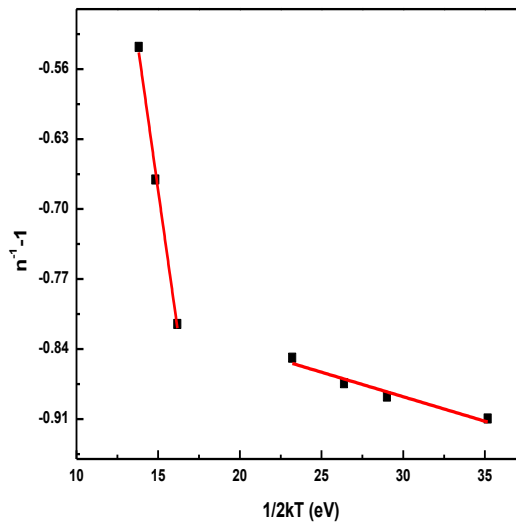


Fig. 5 Ideality factor versus $1/(2kT)$ curves of the Au/n-FS GaNSchottky diode according to two Gaussian distributions of BHs. The data show linear variation in the two temperature ranges with a transition around 240 K.

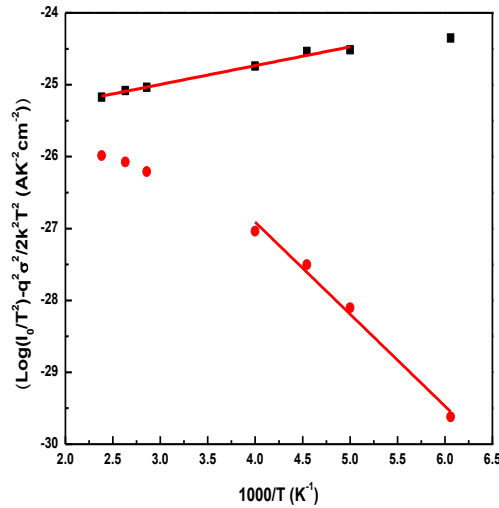


Fig. 6 . Modified Richardson $\ln(I_0/T^2) - (q^2\sigma^2/2k^2T^2)$ versus $1000/T$ plot of the Au/n-FS GaNSchottky barrier diode according to the double GD of BHs for distribution I and II.

It is reported fact that conventional Richardson plot ($1000/T$ versus $\ln AA^*$) plot normally deviate from linearity at low temperature. Therefore according to Gaussian distribution of barrier height, we can write equation for modified Richardson constant as [31],

$$\ln\left(\frac{I_0}{T^2}\right) - \left(\frac{q^2\sigma^2}{2k^2T^2}\right) = \ln(AA^*) - \frac{q\phi_b}{kT} \quad (7)$$

The plot of a modified $\ln(I_0/T^2) - q^2\sigma^2/2k^2T^2$ versus $1000/T$, according to Eq. (7) should give a straight line with the slope directly yielding the mean barrier height and the intercept ($\ln AA^*$) at the ordinate determining A^* for the given diode area A [32]. The $\ln(I_0/T^2) - q^2\sigma^2/2k^2T^2$ versus $1000/T$ values are calculated for both values of σ obtained for the temperature range of 160–240 K (Region I) and 240–450K (Region II) as shown in fig.7. The calculated values of barrier heights and Richardson constants for Region I and II are 0.70 ± 0.01 eV, 1.31 ± 0.01 eV and 21.4, 25.4 $AK^{-2}cm^{-2}$ respectively. The Richardson constant value of 25.4 $AK^{-2}cm^{-2}$ for temperature range 240–450 K is very closer to the theoretical value ($26.4 AK^{-2}cm^{-2}$) in case of n-type GaN.

4. Conclusions

In conclusion, we have investigated the transport characteristics of Au/FS GaN Schottky diodes using double Gaussian distribution model of Schottky barrier heights in the temperature range 160–450 K. The decrease of ideality factor and increase of barrier height demonstrated inhomogenous nature of Au/GaN Schottky diode. The temperature-dependent current–voltage characteristics of the Schottky barrier heights have shown a double Gaussian distribution giving mean BHs of 1.31 ± 0.01 , 0.74 ± 0.01 eV and standard deviations of 0.048 ± 0.001 and 0.013 ± 0.001 eV, respectively. The modified Richardson plot was also drawn to calculated the value of Richardson constant with value 25.4 $AK^{-2}cm^{-2}$. The these results suggest that the experimental data of the Au/FS GaN Schottky diode can be explained by assuming the existence of double Gaussian distribution of the Schottky barrier heights in the wide temperature range.

Acknowledgements

Authors are thankful to Dr. Paul Hagemen, Dr. Hina Ashrf for providing samples. Authors are also thankful to Higher Education Commission, Pakistan for financial support under project No. PM-IPFP/HRD/HEC/2012/3576.

References

- [1] Sung-Woon Moon, John Twynam, Jongsub Lee, Deokwon Seo, Sungdal Jung, Hong Goo Choi, Heejae Shim, Jeong Soon Yim, Sungwon D. Roh, *Solid-State Electronics*. **96**,19 (2014).
- [2] Sunghoon Park, Hyunsung Ko, Soohyun Kim, Chongmu Lee, *Cera. Inter.* **40**,8305 (2014).
- [3] R. Vetry, N.Q. Zhang, S. Keller, U.K. Mishra, *IEEE Trans. Electron Devices* **48**,560 (2001).
- [4] S.C. Jain, M. Willander, J. Narayan, R.V. Overstraeten, *J. Appl. Phys.* **87**,965 (2000).
- [5] H. Ashraf, M. Imran Arshad, S.M Faraz, P. Hagmen, M. Asghar, *J. Apply. Phys.* **108**,103708 (2010).
- [6] Y.J. Lee, J.M. Hwang, T.C. Hsu, M.H. Hsieh, M.J. Jou, B.J. Lee, T.C. Lu, H.C. Kuo, S.C. Wang, *Photon. Technol. Lett. IEEE* **18**,1152 (2006).
- [7] T. Miyajima, T. Tojyo, T. Asano, K. Yanashima, S. Kijima, T. Hino, M. Takeya, S. Uchida, S. Tomiya, K. Funato, T. Asatsuma, T. Kobayashi, M. Ikeda, *J. Phys.: Condens. Matter* **13**,7099 (2001).
- [8] J.C. Carrano, D.J.H. Lambert, C.J. Eiting, C.J. Collins, T. Li, S. Wang, B. Yang, A.L. Beck, R.D. Dupuis, J.C. Campbell, *Appl. Phys. Lett.* **76**,924 (1999).
- [9] F. Tian, E.F. Chor, *Phys. Status Solidi C* **5**,1953 (2008).
- [10] L.S. Chuah, Z. Hassan, H. Abu Hassan, N.M. Ahmed, *J. Alloys Compd.* **481**,L15 (2009).
- [11] O. Menard, F. Cayrel, E. Collard, D. Alquier, *Phys. Status Solidi C* **7**, 112 (2010).
- [12] V. Rajagopal Reddy, V. Janardhanam, Chang-Hyun Leem, Chel-Jong Choi, *Superlattice. Microstruct.* **67**,242 (2014).
- [13] M. Siva Pratap Reddy, A. Ashok Kumar, V. Rajagopal Reddy, *Thin Solid Films* **519**,3844 (2011).
- [14] S. Huang, B. Shen, M.J. Wang, F.J. Xu, Y. Wang, H.Y. Yang, F. Lin, L. Lu, Z.P. Chen, Z.X. Qin, Z.J. Yang, G.Y. Zhang, *App. Phys. Lett.* **91**,072109 (2007).
- [15] B. Roula, T. N. Bhat, Mahesh Kumara, Mohana K. Rajpalke, Neeraj Sinha, A.T. Kalghatgi, S.B. Krupanidhi, *Solid Stat. Commun.* **151**,1420 (2011).
- [16] K. Rao Peta, Byung-Guon Park, Sang-Tae Lee, Moon-Deock Kim, Jae-Eung Oh Tae-Geun Kim, V. Rajagopal Reddy, *Thin Solid Films* **534**,603 (2013).
- [17] S. Monza Faraz, Q. Wahab, M. Imran Arshad, *Semi. Cond. Sci. Tech.* **25**, 095008 (2010).
- [18] M. Asghar, K. Mahmood, M-A Hasan, I. Ferguson, R. Tsu, M. Willander, *Chin. Phys. B* **23**, 097101 (2014).
- [19] M. Asghar, K. Mahmood, A. Ali, M-A Hasan, *Key Eng. Mater.* **510**, 265 (2012).
- [20] S. Chand, J. Kumar, *Appl. Phys. A Mater. Sci. Process.* **65**,497 (1997).
- [21] Nezir Yildirim, Abdilmecit Turut, Veyis Turut, *Microelectronic Eng.* **87**,2225 (2010).
- [22] M. Ravinandan, P. Koteswara Rao, V. Rajagopal Reddy, *Semicond. Sci. Technol.* **24**, 035004 (2009).
- [25] S. Chand and S. Bala, *Appl. Surf. Sci.* **252**,358 (2005).
- [26] K. Cheung and N. W. Cheng, *Appl. Phys. Lett.* **49**,85 (1986).
- [27] S. Zhu, R.L. Van Meirhaeghe, C. Detavernier, F. Cardon, G.P. Ru, X.P. Qu, B.Z. Li, *Solid-State Electron.* **44**,663 (2000).
- [28] S. Chand, J. Kumar, *Semicond. Sci. Technol.* **11**,1203 (1996).
- [29] J. H. Werner, H.H. Guttler, *J. Appl. Phys.* **69**,1522 (1991).
- [30] R. Tung, *Phys. Rev. B* **45**,13509 (1992).
- [31] Y.P. Song, R.L. Vanmeirhaeghe, W.H. Laflere, F. Cardon, *Solid State Electron.* **29**,633 (1986).